Folch, J., Lees, M., & Sloane-Stanley, G. H. (1957) *J. Biol. Chem. 226*, 497.
Gally, H. U., Niederberger, W., & Seelig, J. (1975) *Biochemistry 14*, 3647.
Gally, H. U., Pluschke, G., Overath, P., & Seelig, J. (1979) *Biochemistry 18*, 5605.
Gupta, C. M., Radhakrishnan, R., & Khorana, H. G. (1977) *Proc. Natl. Acad. Sci. U.S.A. 74*, 4315.
Hitchcock, P. B., Mason, R., Thomas, K. M., & Shipley, G. G. (1974) *Proc. Natl. Acad. Sci. U.S.A. 71*, 3036.
Kang, S. Y., Gutowsky, H. S., & Oldfield, E. (1979) *Biochemistry 18*, 3268.
Koul, O., Chou, K., & Jungalwala, F. B. (1980) *Biochem. J. 186*, 959.
Mendelsohn, R., Dluhy, R., Curatolo, W., & Sears, B. (1982) *Chem. Phys. Lipids 30*, 287.
Oldfield, E., Meadows, M., & Glaser, M. (1976) *J. Biol. Chem. 251*, 6147.
Oldfield, E., Gilmore, R., Glaser, M., Gutowsky, H. S., Hshung, J. C., Kang, S. Y., King, T. E., Meadows, M., & Rice, D. (1978a) *Proc. Natl. Acad. Sci. U.S.A. 75*, 4657.
Oldfield, E., Meadows, M., Rice, D., & Jacobs, R. (1978b) *Biochemistry 17*, 2727.
Paddy, M. R., Dahlquist, F. W., Davis, J. H., & Bloom, M. (1981) *Biochemistry 20*, 3152.
Pearson, R. H., & Pascher, I. (1979) *Nature (London) 281*, 499.
Sears, B., Hutton, W. C., & Thompson, T. E. (1976) *Biochemistry 15*, 1635.
Sears, B., Neuringer, L. J., Curatolo, W., & Jungalwala, F. B. (1980) *Fed. Proc., Fed. Am. Soc. Exp. Biol. 39*, 1833.
Seelig, J. (1977) *Q. Rev. Biophys. 10*, 353.
Seelig, A., & Seelig, J. (1974) *Biochemistry 13*, 4839.
Seelig, J., & Gally, H. U. (1976) *Biochemistry 15*, 5199.
Seelig, J., Gally, H. U., & Wohlgemuth, R. (1977) *Biochim. Biophys. Acta 467*, 109.
Seelig, J., Tamm, L., Hymel, L., & Fleischer, S. (1981) *Biochemistry 20*, 3922.
Skarjune, R., & Oldfield, E. (1979) *Biochemistry 18*, 5903.
Smith, M. E. (1968) *Biochim. Biophys. Acta 164*, 285.
Smith, M. E., & Curtis, B. M. (1979) *J. Neurochem. 33*, 447.
Stark, R. E., Manstein, J. L., Curatolo, W., & Sears, B. (1983) *Biochemistry 22*, 2486.
Stockton, G. W., Johnson, K. G., Butler, K. W., Tulloch, A. P., Boulanger, Y., Smith, I. C. P., Davis, J. H., & Bloom, M. (1977) *Nature (London) 269*, 267.
Tamm, L. K., & Seelig, J. (1983) *Biochemistry 22*, 1474.
Toews, A. D., Horrocks, L. A., & King, J. S. (1976) *J. Neurochem. 27*, 25.
Yang, S. F. (1969) *Methods Enzymol. 14*, 208.

Second-Derivative Infrared Spectroscopic Studies of the Secondary Structures of Bacteriorhodopsin and Ca^{2+}-ATPase†

David C. Lee,‡ James A. Hayward,‡,§ Colin J. Restall,‡ and Dennis Chapman*,‡
Departments of Biochemistry and Chemistry, Royal Free Hospital School of Medicine, University of London, London NW3 2PF, U.K., and Department of Biochemistry, State University of New York, Stony Brook, New York 11794
Received December 18, 1984

ABSTRACT: The resolution of minor amide components in the infrared spectra of membrane proteins has, in the past, been limited by the small differences in frequency compared to the large half-widths of the bands that are assigned to different secondary conformations. Here, second-derivative calculations are used to resolve the relatively weak bands that are associated with the β-sheet conformation and the vibrations of some amino acid side chains in the infrared spectra of bacteriorhodopsin and Ca^{2+}-activated adenosine-5′-triphosphatase (Ca^{2+}-ATPase). The spectra presented indicate that bacteriorhodopsin in the purple membrane contains an appreciable amount of β structure in addition to the predominant α_{II}-helical structure. Both sarcoplasmic reticulum and purified Ca^{2+}-ATPase in native lipids contain α-helical and random coil conformations together with a small amount of β structure. In 1,2-dimyristoyl-*sn*-glycero-3-phosphocholine (DMPC) Ca^{2+}-ATPase adopts a secondary conformation similar to that in the sarcoplasmic reticulum, and this structure is unaffected by the phospholipid phase transition. A shift to a predominantly random coil conformation is associated with solubilization of both bacteriorhodopsin and Ca^{2+}-ATPase in 20% Triton X-100. Second-derivative analysis of the carbonyl stretching vibrations of DMPC bilayers indicates that below the phase-transition temperature (T_m) both bacteriorhodopsin and Ca^{2+}-ATPase perturb the interface region such that the *sn*-2 carbonyls adopt a conformation similar to the *sn*-1 carbonyls. Above T_m, these integral proteins have no effect on the static order of the interface region, and the conformational inequivalence of the *sn*-1 and *sn*-2 carbonyls is similar to that found in a pure lipid bilayer.

Infrared (IR)[1] spectroscopy is an established technique for the study of the structures of polypeptides and proteins. The IR-active amide bands are associated with the –CONH– grouping that these molecules have in common. Initial qualitative studies related the frequencies of the relatively

† This work was supported by the Science and Engineering Research Council (D.C.L.), the Muscular Dystrophy Association (J.A.H.), the Commission of the European Communities (C.J.R.), the Wellcome Trust (D.C.), and the Humane Research Trust.
‡ University of London.
§ State University of New York.

[1] Abbreviations: ATP, adenosine 5′-triphosphate; Ca^{2+}-ATPase, Ca^{2+}-activated adenosine-5′-triphosphatase; CD, circular dichroism; DMPC, 1,2-dimyristoyl-*sn*-glycero-3-phosphocholine; DTT, dithiothreitol; HEPES, *N*-(2-hydroxyethyl)piperazine-*N*′-2-ethanesulfonic acid; IR, infrared; M_r, relative molecular weight; SR, sarcoplasmic reticulum; T_m, midpoint temperature of the gel to liquid-crystalline phase transition of a hydrated phospholipid or phospholipid/protein recombinant; Tris, tris(hydroxymethyl)aminomethane.

0006-2960/85/0424-4364$01.50/0

strong amide I and amide II bands to the presence of specific types of secondary structure in various soluble polypeptides and proteins (Krimm, 1962; Susi et al., 1967; Susi, 1969). These amide bands may not be described by a single displacement coordinate, but the amide I band (1700–1600 cm^{-1}) is essentially an in-plane C=O stretching vibration weakly coupled with C–N stretching and in-plane N–H bending (Susi, 1969). The amide II band (1570–1510 cm^{-1}) may be described as an in-plane N–H bending vibration strongly coupled to C–N stretching (Susi, 1969). Early analyses of secondary structure via these absorptions were restricted to samples in the solid state and in ^2H_2O solution because of strong overlapping water absorptions. The advent of microprocessor-controlled IR spectroscopy has permitted the digital subtraction of overlapping water absorptions from the spectra of aqueous samples (Cameron et al., 1979; Chapman et al., 1980).

In principle, a globular protein containing several types of substructure will give several amide I maxima. However, the large half-widths of these components prevent their resolution by even the most powerful spectrometers. Least-squares optimization and Fourier deconvolution procedures have been used for the analysis of overlapping bands (Frazer & Suzuki, 1966; Ruegg et al., 1975; Jap et al., 1983; Mendelsohn et al., 1984). The usefulness of least-squares calculations is limited by the requirement for extensive input information. Typically, the number and peak frequencies of the component bands are required, together with their line shapes, the half-widths, and a linear base line. An alternative method for assessing the number and position of component peaks is derivative spectroscopy. Calculation of the second- and fourth-derivative IR spectra of commercial polymers has permitted the accurate measurement of component peaks and confirmed the curve-fitting calculations (Maddams & Tooke, 1982). Second-derivative IR spectra of water-soluble proteins have recently been obtained (Susi & Byler, 1983). These authors were able to resolve peaks associated with α-helical, β-sheet, and β-turn conformations together with the vibrations of some amino acid side chains.

A number of laboratories are now investigating the structure of membrane proteins using IR spectroscopy (Rothschild & Clark, 1979; Cortijo et al., 1982; Lavialle et al., 1982; Mendelsohn et al., 1984). Our interest has centered on the extent to which lipid dynamics affect the structure of the integral proteins bacteriorhodopsin and Ca^{2+}-ATPase in natural and reconstituted systems (Cortijo et al., 1982; Lee et al., 1984; Restall et al., 1984).

The structure of bacteriorhodopsin is generally accepted to consist of seven transmembrane α-helical rods (Henderson & Unwin, 1975; Engelman et al., 1980). However, recent IR and circular dichroism (CD) spectroscopic studies have suggested the presence of up to four strands of antiparallel β-sheet (Cortijo et al., 1982; Jap et al., 1983). Here, we provide a more detailed analysis, using second-derivative calculations, of IR spectra obtained from H_2O and ^2H_2O preparations. In addition, the stability of the protein structure to changes in temperature and lipid fluidity is investigated in the purple membrane and in a reconstituted system.

The structure of Ca^{2+}-ATPase is studied in three environments: isolated sarcoplasmic reticulum (SR), vesicles of purified ATPase in SR lipids, and reconstituted in a single pure lipid bilayer whose fluidity may be varied. An earlier IR study of this protein suggested that the structure was comprised of α-helical and random coil conformations, but their relative proportions were unknown (Cortijo et al., 1982). CD (Dean & Tanford, 1978; le Maire et al., 1976) and X-ray diffraction (Herbette et al., 1977) studies have revealed a predominantly α-helical conformation. A recent Fourier deconvolution analysis of the IR spectra of SR vesicles revealed amide I shoulders, which were assigned to β structure (Mendelsohn et al., 1984). Here, we apply our second-derivative analysis to the IR spectra and monitor alterations in protein structure induced by changes in temperature and lipid fluidity. Initially, we demonstrate how the overlapping absorptions of atmospheric water vapor may lead to erroneous interpretation of the amide I and amide II peak frequencies. The appearance of sharp features in difference spectra of proteins (Lee et al., 1984; Vincent et al., 1984) may be due to these absorptions.

Materials and Methods

1,2-Dimyristoyl-*sn*-glycero-3-phosphocholine (DMPC) was obtained from Fluka (Glossop, Derbyshire) and its purity confirmed by thin-layer chromatography and differential scanning calorimetry. It was used without further purification. All other materials were of reagent grade.

Purification of Membrane Proteins. SR was isolated from the white muscles of rabbit by the method described by Nakamura et al. (1976). Ca^{2+}-ATPase was purified from SR vesicles essentially as described by Warren et al. (1975). Protein prepared by this method was assumed to be more than 95% pure (Warren et al., 1975) and to have a M_r of 105 000.

Halobacterium halobium (R_1 strain) was grown on a complex medium of salt and bacteriological peptone as described by Oesterhelt & Hartman (1979). Purple membrane was purified according to the method of Oesterhelt & Stoeckenius (1974). Two purification steps were carried out in linear sucrose density gradients (30%–60% w/v) to ensure complete resolution of purple and red membranes. Purple membrane was washed 3 times in distilled water by centrifugation (100000*g* for 30 min) and stored at 4 °C. In preparation for deuterium exchange and IR spectroscopy, SR vesicles and purple membrane were washed twice by centrifugation and resuspended in 10 mM HEPES, 50 mM sucrose, and 1 M KCl, pH 7.4.

Deuterium Exchange and Detergent Solubilization of Membranes. Samples in ^2H_2O were prepared by dialyzing purple membranes or SR vesicles in HEPES H_2O buffer against four changes each of 10 volumes of 10 mM HEPES, 50 mM sucrose, and 1 M KCl, p^{2}H 7.0, in ^2H_2O over 48 h at 4 °C. The p^{2}H of the buffer was adjusted to 7.0 with NaO^2H to yield the deuteron concentration equivalent to the proton concentration in water at pH 7.4 (Glasoe & Long, 1960).

For detergent solubilization, purple membranes (8 mg of protein) were resuspended in 2 mL of 20% v/v Triton X-100 in water, and the mixture was stirred gently for 24 h in the dark at room temperature. Nonsoluble material was removed by centrifugation at 80000*g* for 40 min. The supernatant was used without further modification. Solubilization of SR was carried out in 20% v/v Triton X-100 in HEPES buffer, pH 7.4, by stirring for 2 h at room temperature. Nonsolubilized material was removed by centrifugation as for purple membrane.

Preparation of Reconstituted Systems. Purified Ca^{2+}-ATPase was reconstituted with DMPC according to the method of Gomez-Fernandez et al. (1980). For the first substitution 2 mg of DMPC/mg of protein was used, and in the second substitution 3 mg of DMPC/mg of protein was used. Sodium cholate was added to a final concentration of 1 mg/mg of protein in each substitution step.

Bacteriorhodopsin was reconstituted into DMPC vesicles by performing the above procedure with purified purple

membrane (Alonso et al., 1982). The buffer used in all steps was 150 mM KCl and 20 mM sodium acetate, pH 5.0, and sucrose gradients were made up in this buffer. The level of cholate used in the first substitution was 1 mg/mg of bacteriorhodopsin, and it was 0.8 mg/mg in the second substitution.

The recombinants formed two bands on the linear sucrose density gradient. In each case the lower of these two bands (with the lower lipid to protein ratio) was removed, washed 3 times, and resuspended in HEPES–H_2O buffer.

Analytical Methods. Protein concentration was assayed by the method of Lowry et al. (1951), using bovine serum albumin (Sigma) as the standard. The lipid compositions of the reconstituted systems were assayed by gas–liquid chromatography according to Gomez-Fernandez et al. (1980). Lipid phosphorus concentrations were determined by the method of Rouser et al. (1970); NaH_2PO_4 and adenosine 5′-monophosphate (AMP) served as standards. ATPase activities were measured according to Madden et al. (1979).

Infrared Spectroscopy. All samples for IR spectroscopy were resuspended in 10 mM HEPES, 50 mM sucrose, and 1 M KCl, pH 7.4. Samples were placed in a thermostated Beckman FH-01 CFT microcell with CaF_2 windows and a 7-μm tin spacer. The temperature of the sample was controlled by means of a cell jacket of clrculating water. Temperature calibration, via a thermocouple placed against a cell window, was better than 0.5 °C. Buffers and natural and reconstituted membrane samples were scanned in a Perkin-Elmer IR681 IR spectrometer using a Perkin-Elmer Model 3600 data station for data acquisition and analysis (Cortijo et al., 1982). Ten scans were signal averaged from 1800 or 1750 to 1500 cm^{-1}. The maximum noise filtering of the spectrometer was used together with the widest slit to give a resolution of 3.0 cm^{-1}. Spectral reproducibility was better than 1.0 cm^{-1}. During data acquisition, the spectrometer was continuously purged with dry air at a dew point of −40 °C and a flow rate of 100 L/min. Buffer spectra were recorded in the same cell and under the same temperature and scanning conditions as the corresponding sample spectra. Spectra were recorded at various temperatures by equilibrating the sample at the chosen temperature for 15 min prior to data acquisition, which itself took 48 min. Temperatures were always changed in the direction of increasing temperature. Difference spectra were generated by subtraction of buffer spectra from sample spectra by using the interactive difference routine of the data station. The best subtraction factor was judged by eye to yield a level base line through the region of the broad aqueous water absorption centered at 1645 cm^{-1}. Second-derivative spectra were generated from difference spectra by using an OBEY program available from Perkin-Elmer. The calculations performed by this program correspond to those already described by Susi & Byler (1983).

RESULTS

Absorption of Water Vapor in the Amide I/II Spectral Region. In order to illustrate the difficulties that may be encountered in the detailed analysis of protein structure via amide I and amide II band frequencies, we present (in Figure 1) difference and second-derivative IR spectra of SR recorded in the presence and absence of a continuous purge of dry air. Leaving aside the assessment of protein structure, which will be considered below, we will concentrate for the moment on the contributions of water vapor absorptions to the spectra. Three main absorption bands are seen in the difference spectra of SR (Figure 1a). These are a phospholipid carbonyl stretching absorption at 1735 cm^{-1} and amide I and amide II

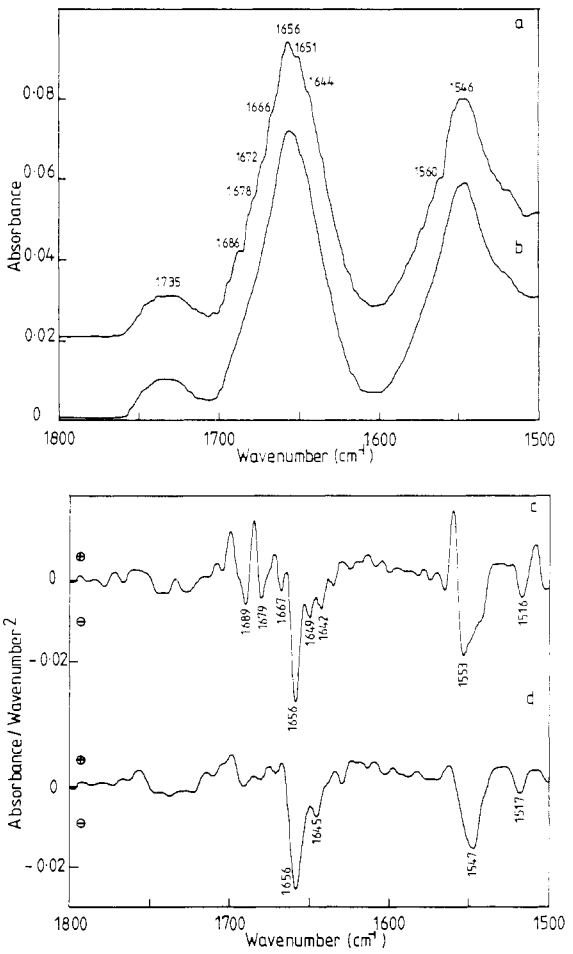

FIGURE 1: Difference (a and b) and second-derivative (c and d) IR spectra in the amide I and II region of sarcoplasmic reticulum at 21 °C recorded under atmospheric (a and c) and dry air purged (b and d) conditions. SR was suspended in 10 mM HEPES, 50 mM sucrose, and 1 M KCl, pH 7.4. The dew point of the air for purging was −40 °C.

bands at 1656 and 1546 cm^{-1}, respectively. It is apparent that purging removes several amide I band shoulders that are seen in the spectrum recorded under atmospheric conditions. These shoulders occur at 1686, 1678, 1672, 1666, 1651, and 1644 cm^{-1}. In addition, an amide II band shoulder, present at 1560 cm^{-1} under atmospheric conditions, is absent on purging. By reference to the tables of Cole (1977) we are able to assign each of these absorptions to H–O–H bending vibrations of atmospheric water vapor. Thus it appears that although the broad amide bands of a complex globular protein are composed of overlapping protein absorptions, great care must be taken in assignment of band shoulders to specific protein structural features. Figure 1b shows second-derivative spectra calculated from the difference spectra presented in Figure 1a. In the second-derivative spectrum, the presence of a negative band corresponds to a positive absorption band in the original difference spectrum. The weak bands at 1667, 1649, and 1642 cm^{-1} are removed on purging and may be assigned to atmospheric water vapor. In addition, a considerable reduction in band intensities occurs at 1689 and 1679 cm^{-1}. The amide II band shifts from 1553 to 1547 cm^{-1} on purging through the removal of the strong water vapor absorption at 1554 cm^{-1}.

Membrane Protein Structure. Our IR investigation of the structure of bacteriorhodopsin in the purple membrane is summarized in Figure 2. In H_2O buffer the difference spectrum at 21 °C shows the amide I band at 1662 cm^{-1} with a shoulder at 1638 cm^{-1} and the amide II band at 1547 cm^{-1}

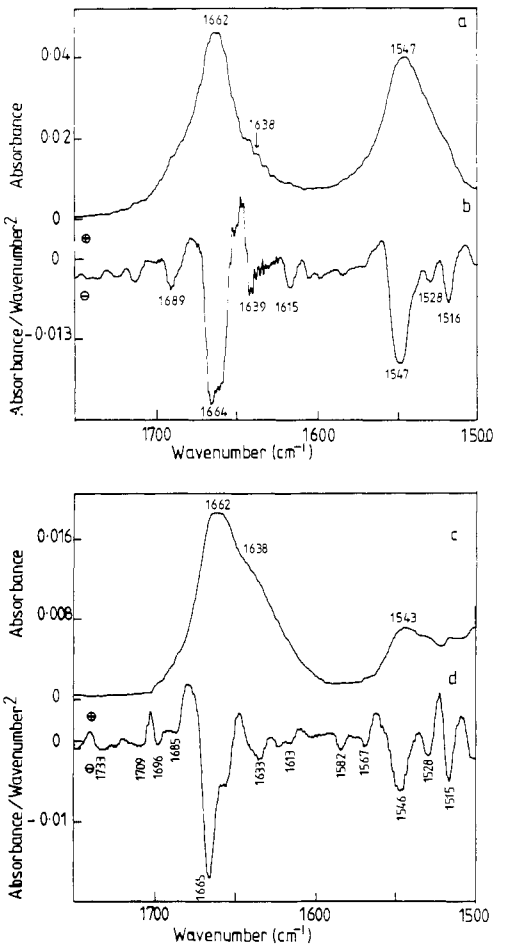

FIGURE 2: Difference (a and c) and second-derivative (b and d) IR spectra in the amide I and II region of purple membrane in H_2O (a and b) and ^2H_2O (c and d), in HEPES buffer at pH 7.4 and p^{2}H 7.0 and 21 °C. Spectra were recorded during a continuous purge of dry air (dew point, −40 °C).

(Figure 2a). The second-derivative spectrum generated from this difference spectrum is presented in Figure 2b. Amide I band components are revealed at 1689, 1664, 1639, and 1615 cm^{-1}. The amide II band is composed of absorptions at 1547, 1528, and 1516 cm^{-1}. The amide I band maximum at 1662 cm^{-1} has been assigned to the presence of distorted α-helices in this protein (Rothschild & Clark, 1979; Cortijo et al., 1982). Krimm & Dwivedi (1982) assign this unusual amide I band frequency to the α_{II}-helix. The position of the amide II band at 1547 cm^{-1} is also indicative of a high proportion of α-helical structure (Thomas & Kyogoku, 1977). However, second-derivative spectroscopy, revealing amide I band components at 1689 and 1639 cm^{-1} (Figure 2b), suggests that a significant proportion of antiparallel β-sheet is also present (Susi et al., 1967; Susi & Byler, 1983). On deuterium substitution (Figure 2c) the most apparent change is a reduction in the amide II to amide I band intensity ratio (A_{II}/A_I), which falls from 0.78 in H_2O buffer to 0.21 in ^2H_2O. This is a reflection of isotopic substitution of the peptide bond N–H to N–^{2}H, which shifts the amide II′ band to lower frequencies. The difference spectrum of the deuterium-exchanged sample shows the amide I′ band at 1662 cm^{-1} with a shoulder at approximately 1638 cm^{-1} and the amide II′ band at 1543 cm^{-1}. The second-derivative spectrum (Figure 2d) contains strong amide I′ and amide II′ components at 1665 and 1546 cm^{-1}, respectively, confirming that the protein is predominantly α-helical. The bands at 1633 and 1528 cm^{-1} suggest the presence of some β-sheet, and the 1685-cm^{-1} band indicates that a proportion of this is antiparallel (Krimm, 1962). In addition, the band at 1696 cm^{-1} may reflect contributions by β-turn structures (Kawai & Fasman, 1978) although this band was not observed in H_2O. The band at 1515 cm^{-1} in Figure 2b,d is partly due to random coil and α-helical structure (Krimm, 1962; Thomas & Kyogoku, 1977), but contribution by tyrosine side chains cannot be ruled out (Chirgadze et al., 1975). Other weak bands revealed in the second-derivative spectra may be tentatively assigned to amino acid side chain vibrations (Susi & Byler, 1983). The bands at 1582 and 1567 cm^{-1} in Figure 2d may be due to aspartate and/or arginine and glutamate residues, respectively (Chirgadze et al., 1975). Tyrosine and/or arginine residues may account for the weak absorption at 1613 cm^{-1} (Chirgadze et al., 1975). The absorption maxima at 1733 and 1709 cm^{-1} (Figure 2d) have frequencies too high for amide I′ band components and are due to lipid carbonyl stretching vibrations (Cortijo et al., 1982).

The infrared spectra of purple membrane suspensions in H_2O buffer and ^2H_2O were recorded over the temperature range 10–45 °C (results not shown). The amide I and amide II band maximum frequencies did not change, suggesting that no gross alterations in secondary structure occur over this temperature range. The bands in the second-derivative spectra at 1689 and 1639 cm^{-1}, which we assign to antiparallel β-sheet, were also unaffected by temperature changes. The other weak bands attributable to various amino acid side chain residues (see above) were present in each spectrum. Some minor changes in the peak frequencies of these bands occurred, but the influence of adjacent water vapor absorptions precludes any strong conclusions.

Figure 3 presents an IR spectroscopic study of the native Ca^{2+}-ATPase in SR vesicles. In the sample used for this study the phospholipid:protein molar ratio was 68:1, and the ATPase specific activity was 1.96 IU. Again, these spectra demonstrate the usefulness of second-derivative analysis in making structural assignments for minor amide band components. The amide I band and amide II band maximum frequencies at 1655 and 1547 cm^{-1}, respectively (Figure 3a), indicate that the secondary structure is a mixture of α-helical and random coil conformations, in agreement with an earlier study (Cortijo et al., 1982). On deuterium substitution (Figure 3c) the A_{II}/A_I ratio is reduced from 0.75 to 0.26, and the amide I′ band is found at 1646 cm^{-1} (Figure 3c). This shift to lower frequencies, which does not occur for α-helical structures, confirms the assignment to random coil structure (Susi et al., 1967). However, a purely random coil structure would be expected to give an amide I′ frequency of 1643 cm^{-1} (Susi et al., 1967). Here, the simultaneous presence of α-helical structure shifts the amide I′ band to higher frequencies. The broad band centered at 1730 cm^{-1} in both spectra is a lipid ester carbonyl stretching vibration.

The presence of more than one protein secondary structure is emphasized by the second-derivative spectra (Figure 3b,d). In ^2H_2O buffer the amide I′ band components may be assigned to α-helical (1656 cm^{-1}), random coil (1642 cm^{-1}), and β-sheet (1631 cm^{-1}) structures (Susi, 1969). The amide II′ band components at 1545 and 1515 cm^{-1} may be assigned to α-helical and random coil structures. The bands at 1605 and 1584 cm^{-1} and the shoulder at 1567 cm^{-1} (Figure 3d) may be tentatively assigned to arginine, aspartate, and glutamine residues, each of which are present in the primary structure in large proportions (Allen et al., 1980). When the second-derivative spectra of SR in H_2O and ^2H_2O buffers are compared, the immediate observation is the greater amount of fine structure in the former. This is undoubtedly due to the rel-

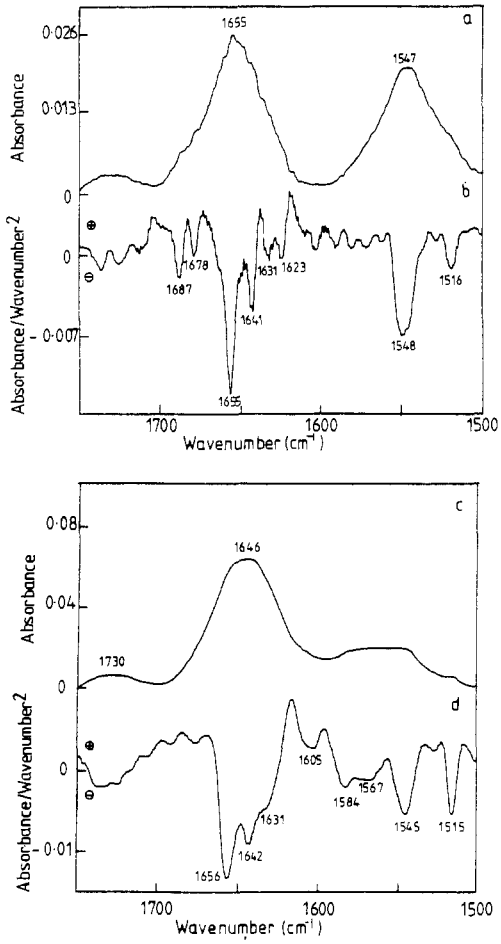

FIGURE 3: Difference (a and c) and second-derivative (b and d) IR spectra in the amide I and II region of sarcoplasmic reticulum in H_2O (a and b) and ^2H_2O (c and d), in HEPES buffer at pH 7.4 and p^{2}H 7.0 at 21 °C. Spectra were recorded during a continuous purge of dry air (dew point, −40 °C).

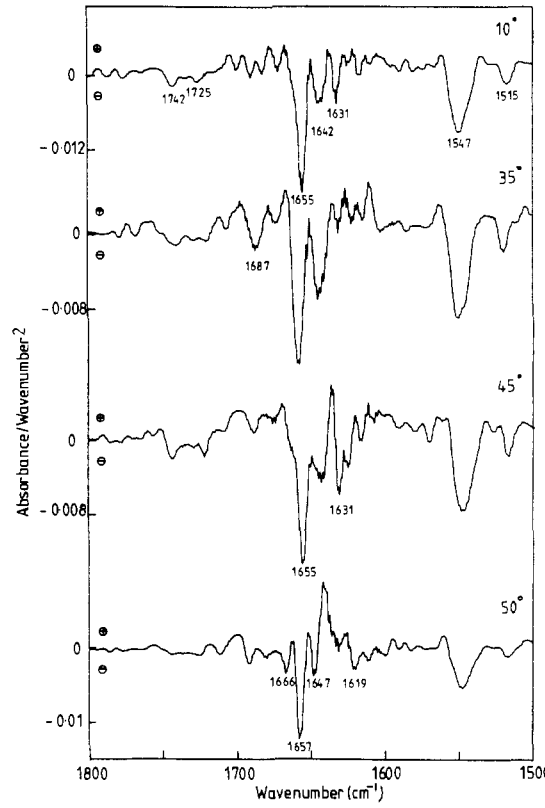

FIGURE 4: The temperature dependence of the second-derivative IR spectra in the amide I and II region of Ca^{2+}-ATPase purified in SR lipids. Purified protein was resuspended in HEPES buffer, pH 7.4. Spectra were recorded during a continuous purge of dry air (dew point, −40 °C).

atively greater influence of water vapor absorption in Figure 3a,b. The bands at 1687, 1678, and 1623 cm^{-1} in Figure 3b may be assigned as H–O–H bending vibrations in the vapor phase.

The effect of temperature on the structure of Ca^{2+}-ATPase was studied by recording IR spectra of SR vesicles in both H_2O and ^2H_2O buffers over the temperature range 10–45 °C (results not shown). As we observed for bacteriorhodopsin in the purple membrane, there was no shift in amide I and amide II band maximum frequencies, indicating no gross secondary structure change over this temperature range. In the second-derivative spectra in ^2H_2O buffer, the bands that we ascribe to α-helical, random coil, and β-sheet conformations remain at 1656, 1642, and 1631 cm^{-1} over the entire temperature range studied. The bands that we have assigned to arginine, aspartate, and glutamate residues were present in each spectrum recorded.

Structure of Purified Ca^{2+}-ATPase. Purification of Ca^{2+}-ATPase enables us to investigate the structure of this protein without spectral contributions from the other SR membrane proteins and to assess the influence of an altered lipid:protein ratio on the structure and its sensitivity to temperature. In Figure 4 we present second-derivative IR spectra of purified Ca^{2+}-ATPase in H_2O buffer at 10, 35, 45, and 50 °C. Spectra were also recorded at intermediate temperatures. The sample used for IR spectroscopy had a phospholipid:protein ratio of 93:1 and an ATPase specific activity of 2.93 IU. The main amide I component near 1655 cm^{-1} in all spectra may be assigned to α-helical and random coil conformations. In the amide II region these structures are represented by the 1547- and 1515-cm^{-1} bands. The spectra are very similar to the spectrum of SR presented in Figure 3b, demonstrating that calsequestrin and the calcium binding protein have little influence on the amide region of the SR spectrum. The band at 1642 cm^{-1}, which is stronger than the amino acid side chain absorptions, may be assigned to the $\nu(2\pi/3.6)$ vibration of the α-helices (Thomas & Kyogoku, 1977). This component has not been observed previously for a membrane protein.

There are a number of spectral changes that accompany increasing temperatures. The 1642-cm^{-1} band increases in intensity relative to the 1655-cm^{-1} band as the temperature is increased from 10 to 40 °C. The weak band at 1631 cm^{-1}, which we ascribe to β structure, is to some extent influenced by the adjacent water vapor band at 1636 cm^{-1}, which makes intensity changes difficult to monitor with certainty. However, there is a notable increase in intensity for this amide I component between 35 and 45 °C. The main amide I band remains at 1655 cm^{-1} on heating, until 50 °C when there is shift to 1657 cm^{-1}. This is accompanied by a sharp drop in intensity in the region of the 1631-cm^{-1} band. These spectral changes in the amide I region are not reflected by any marked changes in either peak frequency or relative intensity in the amide II region. The major components remain at 1547 and 1515 cm^{-1} over the temperature range studied.

Effect of Reconstitution with DMPC on Membrane Protein Structure. Reconstitution into a bilayer containing a single lipid component enables us to study the effects of a pure lipid environment and the phospholipid phase transition on the structures of integral proteins. Figure 5 shows second-derivative IR spectra of a DMPC/bacteriorhodopsin recombinant

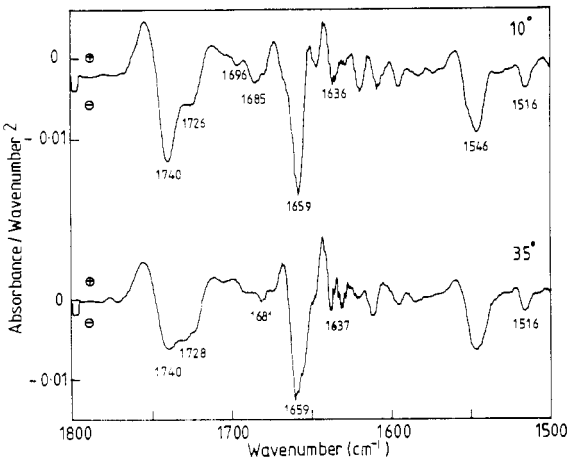

FIGURE 5: Second-derivative IR spectra in the amide I and II region of DMPC/bacteriorhodopsin (molar ratio, 135:1) recorded at the temperatures indicated and in HEPES buffer, pH 7.4. Spectra were recorded during a continuous purge of dry air (dew point, −40 °C).

recorded at temperatures above (35 °C) and below (10 °C) the main phase transition temperature (23 °C). The phospholipid:protein molar ratio of the sample was 135:1. When the spectra are compared with those of purple membrane (Figure 2), it is apparent that there is a shift of the main amide I component from 1664 to 1659 cm^{-1} in the reconstituted system. The band at 1636 cm^{-1}, assigned to β structure, is reduced in both frequency and intensity compared with the spectrum of purple membrane. In addition, the band that we assign to antiparallel β-sheet now appears at 1685 cm^{-1} below T_m. The band at 1696 cm^{-1} is probably due to β-turns. In the amide II region the only major difference between the purple membrane spectrum and that of the reconstituted bacteriorhodopsin is a reduction in intensity at 1528 cm^{-1} that also suggests a reduction in the proportion of β structure. The difference spectra (not shown) gave amide I and II peak maxima at 1659–1660 and 1546 cm^{-1}, respectively, at 10 and 35 °C.

When the sample is heated through the main phase transition, there is no change in the amide I component at 1659 cm^{-1}, suggesting that the secondary structure of the protein is not affected. There is also no change in the positions of the amide II bands at 1546 and 1516 cm^{-1}. These results suggest that the proportions of α-helical and random coil structures are not affected by the change in bilayer fluidity that is characteristic of the phase transition. Also, little alteration in the nature of the β structure is implied by the absence of any major changes at 1685 and 1636 cm^{-1}.

The bands at 1740 and 1726–1728 cm^{-1} are due to C=O stretching vibrations of the fatty acyl–glycerol ester linkages of DMPC (Levin et al., 1982). On passage through the phase transition, we observe a decrease in the intensity of the 1740-cm^{-1} component relative to the 1726–1728-cm^{-1} component. In a pure lipid bilayer, the 1740-cm^{-1} band is characteristic of the carbonyl group of the *sn*-1 chain whose adjacent C_1–C_2 bond is in the trans conformation. The gauche conformation about C_1–C_2 of the *sn*-2 chain produces a carbonyl stretching frequency of 1726 cm^{-1} (Levin et al., 1982).

Figure 6 presents second-derivative IR spectra of Ca^{2+}-ATPase reconstituted in DMPC bilayers recorded at 10, 35, 45, and 50 °C. The phospholipid:protein molar ratio of the sample was 245:1, and the ATPase specific activity was 0.98 IU. The spectra are very similar to those presented for the purified Ca^{2+}-ATPase (Figure 4) and the isolated SR (Figure 3). The main amide I band is at 1655 cm^{-1}, and the amide II band is composed of absorptions at 1546 and 1517 cm^{-1} at

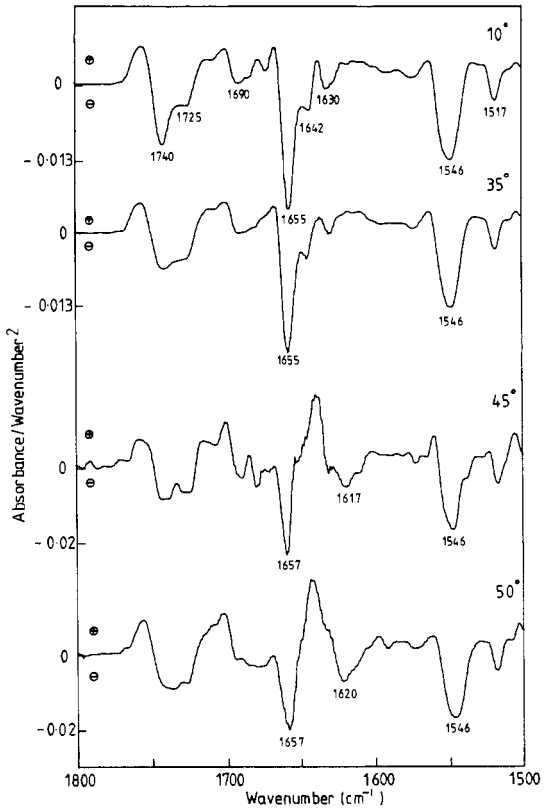

FIGURE 6: The temperature dependence of the second-derivative IR spectra in the amide I and II region of DMPC/Ca^{2+}-ATPase (molar ratio, 245:1) in HEPES buffer, pH 7.4. Spectra were recorded during a continuous purge of dry air (dew point, −40 °C).

Table I: Effect of Intrinsic Proteins on the Intensity Ratio of the Carbonyl Stretching Bands of DMPC

temp (°C)	I_{1726}/I_{1740} DMPC	DMPC/ bacteriorhodopsin (135:1)	DMPC/Ca^{2+}-ATPase (245:1)
10	0.50	0.32	0.31
35	0.79	0.83	0.79

10 °C. These data suggest that the predominantly α-helical and random coil structure of the ATPase is not significantly altered during reconstitution into DMPC bilayers. The bands at 1690 and 1630 cm^{-1} reveal the presence of a small amount of antiparallel β-sheet. The weak band at 1642 cm^{-1} in the spectra recorded at all temperatures from 10 to 40 °C represents the $\nu(2\pi/3.6)$ vibration of α-helical residues. The carbonyl stretching vibrations of the *sn*-1 and *sn*-2 chains of DMPC give rise to the bands at 1740 and 1725 cm^{-1}, respectively.

Table I presents intensity ratio data of the carbonyl stretching bands of liposomes of pure DMPC together with data derived from the spectra shown in Figures 5 and 6. Intensity ratios were calculated by measuring the negative absorbance from zero at 1726 and 1710 cm^{-1} in the second-derivative spectra. For DMPC, the conversion from the gel to liquid-crystalline state produces an decrease in the relative intensity at 1740 cm^{-1}. Incorporation of bacteriorhodopsin or Ca^{2+}-ATPase into the bilayers causes a large reduction in I_{1726}/I_{1740} below T_m. Above T_m, a slight increase in I_{1726}/I_{1740} is observed for the bacteriorhodopsin-containing liposomes and a slight decrease for those containing Ca^{2+}-ATPase. However, these differences are small compared to those observed below T_m.

There are few differences between the spectra recorded at 10 °C and those recorded at 35 °C, suggesting that the phospholipid phase transition has little effect on the secondary structure of Ca^{2+}-ATPase. The structure remains predominantly α-helical (bands at 1655, 1643, and 1546 cm^{-1}) and random coil (bands at 1655 and 1517 cm^{-1}). The small proportion of antiparallel β-sheet is also unaffected—the band intensities at 1690 and 1630 cm^{-1} do not change between 10 and 35 °C. The major difference between these spectra is the decrease in intensity of the C=O stretch at 1740 cm^{-1} relative to the C=O stretch at 1725 cm^{-1}. Spectra recorded at intermediate temperatures (data not shown) confirmed that this change in intensity coincided with the phase transition at around 23 °C. The absence of any alterations in protein secondary structure was also confirmed in these spectra.

Spectra recorded at 40 °C and above showed some significant changes in the secondary structure of Ca^{2+}-ATPase in this reconstituted system. At 40 °C there is an increase in the intensity of the bands that we assign to antiparallel β-sheet at 1690 and 1630 cm^{-1} (not shown). The main amide I and amide II components remain at 1655 and 1546 cm^{-1}, respectively. At 45 °C, however, there is a shift of the amide I band to 1657 cm^{-1} and the appearance of a new band at 1617 cm^{-1}, suggesting a major change in the secondary structure. This is also reflected in a decrease in intensity at 1642 cm^{-1}. There is no change in either peak frequency or relative intensity in the amide II region. A further increase in temperature to 50 °C produces no change in amide I frequency.

Effect of Detergent Solubilization on Membrane Protein Structure. Figure 7 shows difference and second-derivative IR spectra of purple membrane and sarcoplasmic reticulum solubilized in Triton X-100. A high concentration of solubilized protein was obtained by using 20% Triton X-100. Control spectra of 20% Triton X-100 showed that this detergent does not absorb in the spectral region shown. A Triton absorbance at 1610 cm^{-1} prevents accurate interpretation of amide I absorptions below 1620 cm^{-1}. The specific activity of Ca^{2+}-ATPase was reduced to 0.06 IU after solubilization.

The difference spectra (Figure 7a,c) reveal amide I bands at 1656 cm^{-1} for both proteins, suggesting that bacteriorhodopsin and Ca^{2+}-ATPase contain a high proportion of random coil conformation following detergent solubilization. Calculation of the second-derivative spectra provides further details of protein secondary structure. The retention of an appreciable amount of β-sheet structure by bacteriorhodopsin is indicated by the strong band at 1638 cm^{-1} in Figure 7b. The majority of the peptide residues are located in strands of random coil or α-helical conformation as indicated by the main amide I component at 1658 cm^{-1} (Dwivedi & Krimm, 1984; Susi et al., 1967).

In Figure 7d the major amide I component at 1656 cm^{-1} indicates that Ca^{2+}-ATPase adopts a mainly random coil configuration in 20% Triton X-100. The second derivative also reveals bands at 1650 and 1642 cm^{-1}, which are characteristic of α-helical structures. A small amount of antiparallel β-sheet is retained according to the weak bands at 1688 and 1633 cm^{-1}. The shoulder at 1698 cm^{-1} may be due to β-turns. We are unable to assign the bands at 1673 and 1625 cm^{-1} at present. The absorptions at 1736, 1725, and 1715 cm^{-1} are due to lipid carbonyl stretching vibrations.

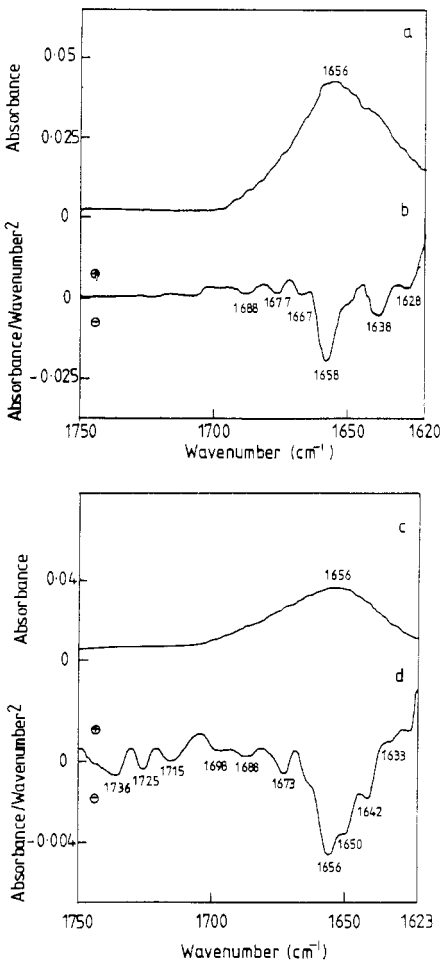

FIGURE 7: Difference (a and c) and second-derivative (b and d) IR spectra in the amide I region of purple membrane (a and b) and sarcoplasmic reticulum (c and d) solubilized in 20% Triton X-100. Purple membrane was solubilized in water and sarcoplasmic reticulum in HEPES buffer, pH 7.4. The spectra were recorded at 21 °C during a continuous purge of dry air (dew point, −40 °C).

DISCUSSION

Second-Derivative IR Spectroscopy. The results presented in this paper describe the first use of second-derivative IR spectroscopy for the analysis of the structure of membrane proteins in aqueous preparations. Second-derivative spectra provide accurate measurements of the peak frequencies of overlapping bands, and these data may be successfully incorporated into the curve-fitting calculations used for quantitative descriptions (Frazer & Suzuki, 1966; Ruegg et al., 1975; Kauppinen et al., 1981; Maddams & Tooke, 1982). In order to obtain quantitative information from second-derivative IR spectra, a number of assumptions must be made. Assuming Lorentzian band shape, the intensity of a second-derivative band is directly proportional to the original intensity and inversely proportional to the square of the half-width (Susi & Byler, 1983). Thus, calculation of the relative proportions of α-helical, random coil, and β-sheet conformations from the relative intensities of the second-derivative peaks assigned to each of these components remains valid only if the half-widths of these bands are identical. Such an assumption is not valid given that different segments of a globular protein are likely to be subject to different restrictions on flexibility and other conformational fluctuations.

A number of features of the second-derivative spectra included here are worthy of general comment. In many cases the major negative amide I component in the second-derivative spectrum appears at higher frequency than the amide I band maximum in the original difference spectrum (Figures 2 and 3). This is due to the removal from the band envelope of the low-frequency β-sheet absorption (1630–1640 cm^{-1}), which now appears as a separate band. This absorption tends to shift the band maximum to lower frequencies in difference spectra

and may lead to mistaken conformational assignments if second-derivative data are not taken into account. Figure 3d provides, to our knowledge, the first resolution of IR absorptions due to α-helical and random coil conformations of a protein in an aqueous system. These conformations could not be resolved by curve-fitting (Ruegg et al., 1975) or second-derivative (Susi & Byler, 1983) analysis of IR spectra of ribonuclease. In addition, the detection of individual side chain vibrations may in future provide specific information on amino acid residues involved in ion pumping or enzyme active sites.

In previous IR studies of protein conformation little attention has been paid to the problem of the overlapping absorptions of atmospheric water vapor in the amide I/II region. Other workers have used a continuous purge of dry nitrogen or air without providing details of the flow rate or the dew point of the air. Indeed, these workers (Lavialle et al., 1982; Vincent et al., 1984) have assigned sharp features on the amide I band envelope to structural features of the proteins concerned. The data presented in Figure 1 provide unambiguous evidence that these features are due to the absorption of atmospheric water vapor. The problem is exacerbated in second-derivative spectra (Figure 1c) because of the emphasis placed on absorptions of narrow bandwidth by the second-derivative method (Maddams & Tooke, 1982). Our earlier study of the perturbations induced by integral polypeptides and proteins in perdeuterated DMPC (Lee et al., 1984) suggested that a conformational change in bacteriorhodopsin could be correlated with the lipid phase transition. However, it was noted that the sharp bands observed in the difference spectra may have been influenced by the absorptions of water vapor.

Membrane Protein Structure. Bacteriorhodopsin exists in a two-dimensional array within the purple membrane of *Halobacterium halobium* (Stoeckenius et al., 1979). This has facilitated the analysis of its structure by electron diffraction and electron microscopy (Henderson & Unwin, 1975). These workers proposed a three-dimensional structure consisting of seven roughly parallel α-helical rods that span the membrane bilayer. Subsequent amino acid sequence analysis, neutron diffraction, and model building studies have led to a detailed description of the disposition of the primary sequence within the seven helices and the arrangement of these helices within the bilayer (Ovchinnikov et al., 1979; Khorana et al., 1979; Engelman et al., 1980; Katre et al., 1981; Keniry et al., 1984). Hayward & Stroud (1981) have obtained electron micrographs to 3.7-Å resolution and proposed a model consisting of four, possibly five, transmembrane α-helices. A recent analysis of these diffraction data, supported by CD and IR spectroscopy, suggested a structure consisting of five α-helices and four transmembrane strands of β-sheet (Jap et al., 1983). These conclusions were based, in part, on least-squares analysis of IR spectra of air-dried films of purple membrane. Our second-derivative analysis of difference IR spectra generated from aqueous samples of purple membrane (Figure 2) provides further evidence for the presence of a significant proportion of antiparallel β-sheet structure, although it is difficult to quantify this for the reasons outlined above. Our IR observation of a small amount of random coil structure is consistent with the allocation of random coil structure to the C-terminus from CD evidence (Wallace & Kohl, 1984).

It has been suggested that the β-sheet domain provides a channel for H^+ transport that overcomes the hydrophobic barrier posed by the membrane (Glaeser & Jap, 1984). Transmembrane α-helices may provide a channel if a water-filled pore is present as has recently been suggested (Plotkin & Sherman, 1984). An alternative mechanism for ion transport is through the provision of a carrier structure that neutralizes the transported proton. Krimm & Dwivedi (1982) argue that the α_{II}-helical structure that they deduce from the IR data may provide such a carrier structure. The proximity of the peptide hydrogens in the α_{II}-helix may facilitate proton transfer along the helical backbone. The shift of the main amide I component that we obtained on reconstitution of bacteriorhodopsin into DMPC vesicles (Figure 5) suggests that the conformation of the α-helices in this system differs from that in the native membrane. However, bacteriorhodopsin that has been reconstituted into DMPC will still pump protons in response to light (Stoeckenius et al., 1979).

Ca^{2+}-ATPase accounts for approximately 95% of the total protein in the SR membrane (Meissner, 1975). Other proteins that are present are "calsequestrin", a calcium binding protein, and proteolipid and glycoprotein fractions (Meissner, 1975). According to our second-derivative IR studies, SR proteins (Figure 3) and purified Ca^{2+}-ATPase (Figure 4) are predominantly α-helical and random coil in structure. This is in agreement with an earlier difference IR study (Cortijo et al., 1982) and a recent Fourier transform IR study (Mendelsohn et al., 1984). CD measurements (le Maire et al., 1976; Dean & Tanford, 1978) and X-ray diffraction (Herbette et al., 1977) also support this conclusion. Our observed amide I frequencies (ca. 1655 cm^{-1} in H_2O buffer and 1642 cm^{-1} in ^2H_2O buffer) indicate that the α-helices are of the α_1 type (Dwivedi & Krimm, 1984). The second-derivative spectra (Figures 3 and 4) also reveal a small amount of antiparallel β-sheet structure in both SR membranes and purified Ca^{2+}-ATPase. The existence of extensive regions of antiparallel β-sheet has been predicted from the primary sequence (Allen et al., 1980). A Fourier deconvolution analysis of IR spectra of SR also suggests the presence of some β structure (Mendelsohn et al., 1984).

The proteins of the SR do not undergo any major conformational changes over the temperature range 10–45 °C according to our IR spectra. The study of the temperature dependence of the structure of purified Ca^{2+}-ATPase reveals some interesting changes (Figure 4). The spectra suggest that there is a significant increase in the proportion of β-sheet structure on increasing the temperature from 35 to 45 °C. A further increase in temperature to 50 °C results in major spectral changes that are indicative of an increase in random coil conformation and a decrease in both α-helical and β-sheet configurations. The conformational changes observed above 45 °C are probably due to protein denaturation and may be associated with the sharp drop in enzyme activity above 48 °C (Inesi et al., 1973). Temperature-dependent spectral changes were also observed by Mendelsohn et al. (1984) for native SR, but these authors did not detect protein denaturation at 50 °C using Fourier deconvolution. It would appear that purification of Ca^{2+}-ATPase from SR renders this protein more susceptible to conformational changes induced by increasing temperature.

The reduction in the amide II/amide I band intensity ratio (A_{II}/A_I) on hydrogen–deuterium exchange of both purple membrane and SR is a common feature of the IR spectra of proteins and, in some cases, may provide information on protein structure (Englander et al., 1982). The reduction in A_{II}/A_I was approximately 70% for both membranes after exchange for 48 h at room temperature, suggesting that the proportion of freely-exchangeable peptide hydrogens is roughly the same for each protein.

Effect of Lipid Dynamics on Integral Protein Structure. Although much is known about the perturbations that integral

proteins cause in their lipid bilayer environment (Chapman, 1982), there is little information concerning the direct effects of lipid fluidity on the structure of integral proteins. The activity of reconstituted Ca^{2+}-ATPase falls dramatically below the T_m of the surrounding lipid (Hesketh et al., 1976). Recently, Fourier transform IR spectroscopy has been used to show that the increase in enzyme activity correlates well with the onset of chain melting in the lipid (Mendelsohn et al., 1984). Below the phase transition, aggregation of the reconstituted Ca^{2+}-ATPase occurs according to freeze–fracture electron microscopy (Gomez-Fernandez et al., 1980). A recent spin-label study is used to argue that, above the phase transition, the activity of Ca^{2+}-ATPase is sensitive to phospholipid structure rather than bilayer fluidity (East et al., 1984). Our second-derivative IR study of the structure of Ca^{2+}-ATPase reconstituted into bilayers of DMPC shows no change in protein secondary structure that can be correlated with the phase transition near 23 °C (Figure 6). This was also observed for bacteriorhodopsin in bilayers of DMPC (Figure 5). At 10 and 35 °C the spectra of the reconstituted Ca^{2+}-ATPase are very similar to those of the purified, native enzyme (Figure 4). Further increases in temperature of the reconstituted enzyme produce changes in secondary structure that mirror those observed for the purified enzyme in native SR lipids at slightly higher temperatures. We conclude that both the lipid to protein ratio (altered on purification) and the nature of the lipid used for reconstitution affect the thermal sensitivity of the protein structure.

While the perturbations induced by integral proteins in the fatty acyl chain and the phosphate head group regions of bilayer lipids have been well characterized by a variety of techniques, there is, at present, little information on structural effects at the interface region located between these two domains. IR spectroscopy and Raman spectroscopy provide an ideal method for studying this problem. The conformational inequivalence about the C_1–C_2 bonds of the *sn*-1 and *sn*-2 acyl chains gives rise to a splitting of the stretching frequencies of the adjacent carbonyl groups (Levin et al., 1982). In this study we find that the presence of the integral proteins in the bilayer reduces the conformational inequivalence below the phase transition so that a proportion of the originally bent *sn*-2 chains are now constrained in a conformation similar to that of the *sn*-1 chain. As a consequence, the perturbed *sn*-2 carbonyls would be displaced toward the center of the bilayer. A similar effect has also been observed on introduction of cholesterol into a pure lipid bilayer below the phase transition (Bush et al., 1980). When the bilayer is heated through the phase transition, this intensity ratio effect is reversed and the conformational inequivalence is restored (Figures 5 and 6). We conclude that, above the phase transition, the integral proteins do not cause any perturbation of static order in the interface region and the C_1–C_2 bonds adopt a trans and gauche conformation in the *sn*-1 and *sn*-2 chains, respectively. Thus, the perturbing effects of integral proteins on the interface region reflect their disruption of the hydrophobic core above and below the transition. Our previous IR studies have shown that, below the phase transition, integral proteins produce a decrease in the static order of the acyl chains whereas above the transition there is no effect on the static order (Cortijo et al., 1982; Lee et al., 1984).

Membrane Protein Structure after Detergent Solubilization. The structure of bacteriorhodopsin in detergent solution is of interest because of the recent formation of crystals from detergent solution (Michel & Oesterhelt, 1980). These workers obtained bacteriorhodopsin in crystal form by salt precipitation after solubilization in octyl glucoside. The secondary structure of the protein in this form is, as yet, unknown. However, purple membrane may be solubilized in 10% Triton X-100, and the native hexagonal lattice of bacteriorhodopsin re-formed upon removal of the detergent according to X-ray diffraction (Cherry et al., 1978).

The IR spectra presented in Figure 7 clearly demonstrate that solubilization in Triton X-100 causes an increase in the proportion of random coil conformation in both bacteriorhodopsin and Ca^{2+}-ATPase. However, both proteins retain some α-helical and β-sheet conformation. A CD study of the conformation of Ca^{2+}-ATPase in deoxycholate also demonstrated a reduction in the α-helical content which accompanied a decrease in enzyme activity (le Maire et al., 1976). This was not observed in a CD study of Ca^{2+}-ATPase in the nonionic detergent $C_{12}E_8$ where enzyme activity was retained (Dean & Tanford, 1978). These authors also demonstrated that enzyme activity could be maximally restored to delipidated Ca^{2+}-ATPase by the addition of 0.1% Triton X-100. The enzyme activity was reduced by 97% after solubilization in 20% Triton X-100, and the large proportion of random coil structure is a reflection of this.

Conclusions

In summary, second-derivative calculations are of great value in the resolution of minor amide I and amide II components from the broad band envelopes and in assigning these absorptions to conformational features. The importance of obtaining an adequate purge with dry gas is emphasized for the accurate interpretation of IR spectra, particularly second-derivative spectra. The spectra demonstrate that both bacteriorhodopsin and Ca^{2+}-ATPase contain antiparallel β-sheet structure in addition to α-helical and random coil structure. The secondary structure of Ca^{2+}-ATPase appears to be unaffected by purification in SR lipids or reconstitution into DMPC bilayers. However, solubilization by Triton X-100 causes conformational changes in both bacteriorhodopsin and Ca^{2+}-ATPase that involve large increases in the proportions of random coil conformations although α-helical and β-sheet forms remain. It was shown that the change in bilayer fluidity which accompanies the phase transition of DMPC has no effect on the secondary structures of either protein in reconstituted systems. However, purification in SR lipids or reconstitution in DMPC bilayers renders the structure of Ca^{2+}-ATPase more sensitive to temperatures above 35 °C.

Second-derivative analysis of the carbonyl stretching bands of DMPC indicates that bacteriorhodopsin and Ca^{2+}-ATPase perturb the static order of the bilayer interface region below T_m but have little effect above T_m. Analysis of these bands should, in future, provide much information on the structure of the interface region and the perturbations caused by integral molecules.

Acknowledgments

We thank Christine Hall for excellent technical assistance.

Registry No. ATPase, 9000-83-3; DMPC, 18194-24-6.

References

Allen, G., Trinnaman, B. J., & Green, N. M. (1980) *Biochem. J. 187*, 591–616.

Alonso, A., Restall, C. J., Turner, M., Gomez-Fernandez, J. C., Goni, F. M., & Chapman, D. (1982) *Biochim. Biophys. Acta 689*, 283–289.

Bush, S. F., Levin, H., & Levin, I. W. (1980) *Chem. Phys. Lipids 27*, 101–111.

Cameron, D. G., Casal, H. L., & Mantsch, H. H. (1979) *J. Biochem. Biophys. Methods 1*, 21–36.

Chapman, D. (1982) *Biol. Membr. 4*, 179–229.
Chapman, D., Gomez-Fernandez, J. C., Goni, F. M., & Barnard, M. (1980) *J. Biochem. Biophys. Methods 2*, 315–323.
Cherry, R. J., Muller, U., Henderson, R., & Heyn, M. P. (1978) *J. Mol. Biol. 121*, 283–298.
Chirgadze, Yu. N., Fedorov, O. V., & Trushina, N. P. (1975) *Biopolymers 14*, 679–694.
Cole, A. R. H. (1977) *Tables of Wavenumbers for the Calibration of Infrared Spectrometers*, International Union of Pure and Applied Chemistry, Pergamon Press, New York.
Cortijo, M., Alonso, A., Gomez-Fernandez, J. C., & Chapman, D. (1982) *J. Mol. Biol. 157*, 597–618.
Dean, W. L., & Tanford, C. (1978) *Biochemistry 17*, 1683–1690.
Dwivedi, A. M., & Krimm, S. (1984) *Biopolymers 23*, 923–943.
East, J. M., Jones, O. T., Simmonds, A. C., & Lee, A. G. (1984) *J. Biol. Chem. 259*, 8070–8071.
Engelman, D. M., Henderson, R., McLachlan, A. D., & Wallace, B. A. (1980) *Proc. Natl. Acad. Sci. U.S.A. 77*, 2023–2027.
Englander, J. J., Downer, N. W., & Englander, S. W. (1982) *J. Biol. Chem. 257*, 7982–7986.
Fraser, R. D. B., & Suzuki, E. (1966) *Anal. Chem. 38*, 1770–1773.
Glaeser, R. M., & Jap, B. K. (1984) *Biophys. J. 45*, 95–97.
Glasoe, P. K., & Long, E. A. (1960) *J. Phys. Chem. 64*, 188–191.
Gomez-Fernandez, J. C., Goni, F. M., Bach, D., Restall, C. J., & Chapman, D. (1980) *Biochim. Biophys. Acta 598*, 502–516.
Hayward, S. B., & Stroud, R. M. (1981) *J. Mol. Biol. 151*, 491–517.
Henderson, R., & Unwin, P. N. T. (1975) *Nature (London) 257*, 28–32.
Herbette, L., Marquardt, J., Scarpa, A., & Blaise, J. K. (1977) *Biophys. J. 20*, 245–272.
Hesketh, T. R., Smith, G. A., Houslay, M. D., McGill, K. A., Birdsall, N. J. M., Metcalfe, J. C., & Warren, G. B. (1976) *Biochemistry 15*, 4145–4151.
Inesi, G., Millman, M., & Eletr, S. (1973) *J. Mol. Biol. 81*, 483–504.
Jap, B. K., Maestre, M. F., Hayward, S. B., & Glaeser, R. M. (1983) *Biophys. J. 43*, 81–89.
Katre, N. V., Wolber, P. K., Stoeckenius, W., & Stroud, R. M. (1981) *Proc. Natl. Acad. Sci. U.S.A. 78*, 4068–4072.
Kauppinen, J. K., Moffat, D. J., Mantsch, H. H., & Cameron, D. G. (1981) *Anal. Chem. 53*, 1454–1457.
Kawai, M., & Fasman, G. (1978) *J. Am. Chem. Soc. 100*, 3630–3632.
Keniry, M. A., Gutowsky, H. S., & Oldfield, E. (1984) *Nature (London) 307*, 383–386.
Khorana, H. G., Gerber, G. E., Herlihy, W. C., Gray, C. P., Anderegg, R. J., Nihei, K., & Bieman, K. (1979) *Proc. Natl. Acad. Sci. U.S.A. 76*, 5046–5050.
Krimm, S. (1962) *J. Mol. Biol. 4*, 528–540.
Krimm, S., & Dwivedi, A. M. (1982) *Science (Washington, D.C.) 216*, 407–408.
Lavialle, F., Adams, R. G., & Levin, I. W. (1982) *Biochemistry 21*, 2305–2312.
Lee, D. C., Durrani, A. A., & Chapman, D. (1984) *Biochim. Biophys. Acta 769*, 49–56.
le Maire, M., Jorgenson, K. E., Roigaard-Petersen, H., & Moller, J. V. (1976) *Biochemistry 15*, 5805–5812.
Levin, I. W., Mushayakarara, E., & Bittman, R. (1982) *J. Raman Spectrosc. 13*, 231–234.
Lowry, O. H., Rosebrough, N. J., Farr, A. L., & Randall, R. J. (1951) *J. Biol. Chem. 193*, 265–275.
Maddams, W. F., & Tooke, P. B. (1982) *J. Macromol. Sci. Chem. A17*, 951–968.
Madden, T. D., Chapman, D., & Quinn, P. J. (1979) *Nature (London) 279*, 538–541.
Meissner, G., (1975) *Biochim. Biophys. Acta 389*, 51–68.
Mendelsohn, R., Anderle, G., Jaworsky, M., Mantsch, H. H., & Dluhy, R. A. (1984) *Biochim. Biophys. Acta 775*, 215–224.
Michel, H., & Oesterhelt, D. (1980) *Proc. Natl. Acad. Sci. U.S.A. 77*, 1283–1285.
Nakamura, H., Jilka, R. L., Boland, R., & Martonosi, N. (1976) *J. Biol. Chem. 251*, 5414–5423.
Oesterhelt, D., & Stoeckenius, W. (1974) *Methods Enzymol. 31*, 667–678.
Oesterhelt, D., & Hartman, R. (1979) in *Membrane Biochemistry* (Carafoli, E., & Semenza, G., Eds.) pp 154–163, Springer, Berlin.
Ovchinnikov, Yu. N., Abdulaev, N. G., Feigina, M. Yu., Kiselev, A. V., & Lobanov, N. A. (1979) *FEBS Lett. 100*, 219–224.
Plotkin, B. J., & Sherman, W. V. (1984) *Biochemistry 23*, 5353–5360.
Restall, C. J., Dale, R. E., Murray, E. K., Gilbert, C. W., & Chapman, D. (1984) *Biochemistry 23*, 6765–6775.
Rothschild, K. J., & Clark, N. A. (1979) *Science (Washington, D.C.) 204*, 311–312.
Rouser, G., Fleischer, S., & Yamamoto, A. (1970) *Lipids 5*, 494–496.
Ruegg, M., Metzger, V., & Susi, H. (1975) *Biopolymers 14*, 1465–1471.
Stoeckenius, W., Lozier, R. H., & Bogomolni, R. A. (1979) *Biochim. Biophys. Acta 505*, 215–278.
Susi, H. (1969) in *Structure and Stability of Biological Macromolecules* (Timasheff, S. N., & Fasman, G. D., Eds.) pp 575–663, Marcel Dekker, New York.
Susi, H., & Byler, D. M. (1983) *Biochem. Biophys. Res. Commun. 115*, 391–397.
Susi, H., Timasheff, S. N., & Stevens, L. (1967) *J. Biol. Chem. 242*, 5460–5466.
Thomas, G. J., & Kyogoku, Y. (1977) *Pract. Spectrosc. 1*, 717–872.
Vincent, J. S., Steer, C. J., & Levin, I. W. (1984) *Biochemistry 23*, 625–631.
Wallace, B. A., & Kohl, N. (1984) *Biochim. Biophys. Acta 777*, 93–98.
Warren, G. B., Toon, P. A., Birdsall, N. J. M., Lee, A. G., & Metcalfe, J. C. (1974) *Proc. Natl. Acad. Sci. U.S.A. 71*, 622–626.